Environmental Science Nano

Interaction of CuO Nanoparticles with Plant Cells: Internalization, Oxidative stress, Electron Transport Chain Disruption, and Toxicogenomic Responses

Journal:	*Environmental Science: Nano*
Manuscript ID	EN-ART-02-2018-000222.R1
Article Type:	Paper
Date Submitted by the Author:	05-Aug-2018
Complete List of Authors:	Dai, Yanhui; Ocean University of China, College of Environmental Science and Engineering Wang, Zhenyu; Jiangnan University Zhao, Jian; Ocean University of China, College of Environmental Science and Engineering Xu, Lili; Ocean University of China, College of Environmental Science and Engineering Xu, Lina; Ocean University of China, College of Environmental Science and Engineering Yu, Xiaoyu; Ocean University of China, College of Environmental Science and Engineering Wei, Yongpeng; Ocean University of China, College of Environmental Science and Engineering Xing, Baoshan; UMASS, Stockbridge School of Agriculture

Environmental Significance

CuO nanoparticles (NPs) have raised environmental concerns due to their relatively high toxicity. Oxidative stress is recognized as a main mechanism for CuO NPs toxicity to plants. However, the origin of cellular reactive oxygen species (ROS) and gene expression related to oxidative stress were poorly understood. Our results showed that the internalized CuO NPs were located on mitochondria of plant (BY-2) cells. CuO NPs could inhibit complexes I and III on mitochondrial electron transport chain (ETC) of plant cells, resulting in the over-generation of ROS and oxidative stress-induced membrane damage. The oxidative stress- and ETC-related genes were further identified by RNA-sequencing. The findings will be helpful for better understanding the phytotoxicity and environmental risk of CuO NPs.

Interaction of CuO Nanoparticles with Plant Cells: Internalization, Oxidative stress, Electron Transport Chain Disruption, and Toxicogenomic Responses

Yanhui Dai,[1] Zhenyu Wang,[2,3] Jian Zhao,[1] Lili Xu,[1] Lina Xu,[1] Xiaoyu Yu,[1] Yongpeng Wei,[1] and Baoshan Xing*,[4]

[1] Institute of Costal Environmental Pollution Control, and Ministry of Education Key Laboratory of Marine Environment and Ecology, Ocean University of China, Qingdao 266100, China

[2] Institute of Environmental Processes and Pollution Control, and School of Environmental and Civil Engineering, Jiangnan University, Wuxi 214122, China

[3] Laboratory for Marine Ecology and Environmental Science, Qingdao National Laboratory for Marine Science and Technology, Qingdao 266071, China

[4] Stockbridge School of Agriculture, University of Massachusetts, Amherst, Massachusetts 01003, United States

*Corresponding author

Tel.: +1 413 545 5212; fax: +1 413 577 0242

E-mail address: bx@umass.edu (Dr. Baoshan Xing)

Abstract

This study investigated the toxicity of CuO nanoparticles (NPs) to *Nicotiana tabacum* L. cv. Bright Yellow-2 (BY-2) cells. CuO NPs higher than 2 mg/L began to exhibit significant inhibition on the growth of plant cells, and the 24-h median effective concentration was calculated as 12 mg/L. CuO NPs (12 mg/L) showed much higher toxicity than the released Cu^{2+} (0.8 mg/L) and bulk particles (BPs, 12 mg/L) during all the exposure times (0-24 h). CuO NPs were internalized by plant cells through endocytosis, and then located in cytoplasm, mitochondria and vacuoles. Under CuO NPs exposure, the generation of total reactive oxygen species increased by 38.3%, and 40.9% compared with CuO BPs, and Cu^{2+} treatments, respectively. The main radical species were identified as H_2O_2 and $OH^{\cdot}$. CuO NPs significantly reduced the activities of complexes I and III on mitochondrial electron transport chain, blocked the electron transfer from NADH to ubiquinone, and from ubisemiquinone to ubiquinol, induced oxidative stress, and finally led to membrane damage as indicated by an increase in the contents of malondialdehyde and lactate dehydrogenase. Global gene expression analysis from RNA-sequencing showed that CuO NPs (12 mg/L) significantly induced 2692 differentially expressed genes (P-value < 0.05, fold-change > 2) including 1132 up-regulated and 1560 down-regulated genes in BY-2 cells. The differentially expressed genes related to oxidative stress and mitochondria were identified according to Gene Ontology (GO) and Kyoto Encyclopedia of Gene and Genomes (KEGG) analysis. This work provides insights into the molecular mechanism of nanotoxicity toward plants.

Keywords:

Nicotiana tabacum; endocytosis; reactive oxygen species; lipid peroxidation; RNA-sequencing

1. Introduction

The broad use of CuO nanoparticles (NPs) and CuO NPs-containing products would lead to increasing release of NPs into the environment,[1] which is a potential threat to the ecosystems. Plants, primary producers in ecosystems, are commonly used for assessing the ecotoxicity and environmental risk. Currently, there are many publications on the interaction of NPs with different plant species such as crops, vegetables and aquatic plants, in which the biological responses of plants caused by NPs were reported.[2-4] Recent studies on plant omics shed further light on the mechanisms (such as oxidative stress and related molecular response) of NPs on plants.[5-7] Interaction of NPs with plant cells could better explain these specific biological responses because plant cells represent the ultimate unit of higher plant.[8] Current investigations on plant cell-NPs interaction showed that oxidative stress was a main mechanism for phytotoxicity.[9] H_2O_2 and $O_2^{\cdot -}$ were recognized as the main reactive oxygen species (ROS) during the exposure of CuO NPs to plants (e.g., *Arabidopsis thaliana*),[10] and the exposure of Al_2O_3 NPs to plant cells, such as *Nicotiana tabacum* L. cv. Bright Yellow-2 (BY-2) cells.[8] But the origin of cellular ROS was poorly identified. Previous publications reported that carbon nanotubes (CNTs) could locate in mitochondria of plant cells,[11] and decreased mitochondrial

activity.[12] Another report found that Al_2O_3 NPs resulted in the loss of mitochondrial potential of BY-2 cells.[8] Mitochondria in plant cells could be a major origin/location for ROS generation, and the over-generation of mitochondrial ROS can be triggered in response to a range of abnormal conditions (e.g., biotic and abiotic stresses) or during the disruption of electron transport chain (ETC) in plant cells.[12,13] We thus hypothesized that CuO NPs could be internalized by plant cells and disrupt mitochondrial ETC through direct contact with mitochondria, thus causing the over-generation of ROS and oxidative stress.

Recent study found that Al_2O_3 NPs had no inhibition on *Arabidopsis* growth, but 148 genes including root-development-related genes and nutrition-related genes were differentially expressed.[14] Therefore, the detection of changes in gene expression upon NPs exposure could bring new insight into the responses of plants prior to any apparent changes in physiology and/or morphology of plants.[15] For the whole plants, Xun et al.[16] reported that the shoot and root of maize displayed the differences in both the number of up- or down-regulated genes and specific categories of gene ontology (GO) terms upon ZnO NPs exposure. However, there is currently no genome-wide investigation or transcriptome analysis on plant cells when exposing to NPs. To further understand the molecular mechanisms controlling oxidative stress induced by CuO NPs, the gene expression related to oxidative stress and mitochondrial functions in plant cells was investigated in this study. In addition, RNA-sequencing (RNA-Seq) is an efficient high-throughput method for gene expression analysis.[3] Therefore, differentially expressed genes in plant cells were identified upon CuO NPs exposure

using RNA-Seq in the present work, and the biological processes involved were further analysed to better explain the relationship between oxidative stress and the disruption of mitochondrial ETC.

In this work, we used BY-2 cells, known as the "Hela" cell of plants, as a model plant cell line. The objectives of this work were to (1) investigate the effect of internalized CuO NPs on the disruption of specific sites of mitochondrial ETC in plant cells, and the relationship between ROS generation and ETC blocking; and (2) explore the differentially expressed genes that respond to oxidative stress, regulate antioxidant enzymatic activities, and relate to mitochondria and mitochondrial ETC. These findings will provide useful information for better understanding the physiological and molecular mechanisms on the adverse effects of CuO NPs to plants.

2. Materials and Methods

2.1 Characterization of CuO NPs and BPs

CuO NPs and bulk particles (BPs) (purity > 99.9%) were purchased from Sigma-Aldrich, and the sizes provided from the manufacturer were < 50 nm, and < 5 μm, respectively. Transmission electron microscopy (TEM, JEM-2100, JEOL, Japan) and scanning electron microscopy (SEM, Nova Nano 450, FEI, USA) were used to characterize the individual size and morphology of CuO NPs and BPs. Surface areas of CuO NPs and BPs were determined by an Autosorb-1C (Quantachrome Instruments Ltd., USA). Zeta potential and hydrodynamic diameter of CuO NPs and BPs (12 mg/L) in 1/2 MS medium (pH 5.8, Table S1) and ultrapure water (pH 5.8) were examined by Nanosizer (Malvern Instruments, Ltd., UK) after sonicating (100 W,

40 kHz) for 20 min. To investigate the dissolution of CuO NPs or BPs in 1/2 MS medium, Cu^{2+} concentrations released from NPs or BPs were determined as a function of incubation times. Briefly, CuO NPs or BPs were suspended in 1/2 MS medium to achieve the final concentration of 10 mg/L. After 0.5, 2, 6, 12, 24, and 36 h, the suspensions were centrifuged at 9,280 ×g for 30 min, and then filtered by a 0.22-μm membrane filter to remove CuO NPs or BPs. The Cu contents in the filtrates were determined by graphite furnace atomic absorption spectrophotometry (GFAAS, Thermo Electron Co., USA).

2.2 Viability of BY-2 cells after CuO NPs exposure

Tobacco BY-2 cells were provided by College of Life Sciences and Oceanography, Shenzhen University. The cells were cultured in 1/2 MS medium and maintained at 25 °C in dark on a shaker (130 rpm) before exposure. Cell viability was indicated by 2, 3, 5-triphenyltetrazolium chloride (TTC, Sigma).[8] Briefly, plant cells (5×10^5 cells/mL) were added into the 24-well plates, and then incubated with CuO NPs at different concentrations (0, 0.2, 0.5, 1, 2, 4, 6, 8, 10, 20, and 50 mg/L) for 24 h. After that, supernatant was removed by centrifugation (120 ×g, 10 min). Cells were resuspended in 0.3% TTC (v/v) which was pre-dissolved in 50 mM phosphate buffer solution (PBS, pH 7.2), and cultured for 10 h. Then, the cells were collected with centrifugation (120 ×g, 10 min), added into 95% ethanol, and heated at 60 °C for 15 min. Cells (200 μL) were transferred into 96-well plates to determine the optical density value at 485 nm by Microplate Reader (Thermo, USA). To investigate the cell viability as a function of exposure times, plant cells (5×10^5 cells/mL) were added into 24-well plates and

treated with CuO NPs (12 mg/L), BPs (12 mg/L) or Cu^{2+} ions (0.8, 9.6 mg/L, supplied as $CuSO_4 \cdot 5H_2O$) for 2, 4, 8, 16, and 24 h. "12 mg/L" was the 24-h median effective concentration (EC_{50}) of CuO NPs as obtained from the cell viability assay. Two Cu^{2+} treatments (0.8 and 9.6 mg/L) were conducted to investigate the effect of the dissolved Cu^{2+} concentration from CuO NPs (12 mg/L) and equal Cu content of CuO NPs (12 mg/L), respectively. Cell viability was determined by the TTC method as mentioned above.

2.3 Endocytosis investigation

Wortmannin was an inhibitor that can block the endocytosis process of plant cells. Wortmannin was dissolved in dimethylsulphoxide (DMSO, Sigma) to prepare its stock solution (1 mM). Cells were mixed with wortmannin solution (33 μM) for 30 min, and then treated with CuO NPs (2, 12 mg/L) for 12 h. The collected cells by centrifugation (120 ×g, 10 min) were washed three times with 20 mM ethylenediamine tetraacetic acid (EDTA) and 20 mM PBS (pH 7.2), respectively. The obtained cells were moved into a digestion vessel. After mixing with 10 mL pure HNO_3, the cell samples were digested for 30 min at a maximum pressure of 180 psi in a microwave system (Mars5, CEM, Matthews, NC, USA). Cu contents in the digestion solutions were then determined by GFAAS.

2.4 TEM observation

TEM was used to observe the morphological changes of BY-2 cells and intracellular distribution of NPs upon CuO NPs exposure. Cells were collected after exposure with CuO NPs for 12 h. The collected cells were washed with EDTA (20

mM), and PBS (20 mM, pH 7.2) three times, and fixed in 3% glutaraldehyde for 12 h. The cells were then washed three times with PBS and post-fixed in 1% osmium tetraoxide. After fixation, the cells were dehydrated in acetone, and embedded in EPON812 resin. The ultrathin sections were made for TEM observation with an energy dispersive spectroscopy (EDS, INCA100, Oxfordshire, UK).

2.5 Reactive oxygen species (ROS) determination

Intracellular total ROS was detected using a fluorescent probe 2', 7'-dichlorofluorescin diacetate (DCFH-DA, Beyotime Institute of Biotechnology, China). After exposure to CuO NPs (12 mg/L), CuO BPs (12 mg/L) and Cu^{2+} (0.8 mg/L) for 0, 1, 2, 4, 8, 16, and 24 h, the cells were collected with centrifugation (120 ×g, 10 min), and then incubated with DCFH-DA (10 μM) in the dark for 30 min. Thereafter, the cells were washed three times with ultrapure water to remove the DCFH-DA. The cells were broken under sonication (120 W, FB120, Fisher Scientific, USA), and then centrifuged (1620 ×g, 10 min) at 4 °C. The relative fluorescence intensity of the supernatant was determined by molecular fluorescence spectrophotometer (F4600, Hitachi, Japan), and the excitation and emission wavelengths were 488 and 530 nm, respectively. As for H_2O_2, hydroxyl radical (OH·), $O_2^{\cdot -}$ detection, the cells were cultured with CuO NPs (12 mg/L), CuO BPs (12 mg/L), and Cu^{2+} (0.8 mg/L) for 4 h. The collected cells were then broken and centrifuged (1620 ×g, 10 min) at 4 °C for determination by an assay kit (Jiancheng, Nanjing, China) following the manufacturer's instructions. Detailed information was shown in Supplementary Information (SI).

2.6 Antioxidant enzyme activity, lipid peroxidation and lactate dehydrogenase determination

Cells were cultured with CuO NPs (12 mg/L), CuO BPs (12 mg/L), and Cu^{2+} (0.8 mg/L) for 4 h. Then the cells were collected by centrifugation (120 ×g, 10 min) to determine the activities of catalase (CAT), superoxide dismutase (SOD), malondialdehyde (MDA). The release of lactate dehydrogenase (LDH) in the supernatants was also detected. CAT and SOD activities were analyzed by an assay kit (Jiancheng, Nanjing, China) following the manufacturer's instructions. MDA contents were obtained from the standard curve following the instructions of lipid peroxidation MDA assay kit (Beyotime Institute of Biotechnology, China). LDH activity was detected by LDH Cytotoxicity Assay Kit (Beyotime Institute of Biotechnology, China) according to the manufacturer's instructions. Detailed procedures for the assays of SOD, CAT, MDA, LDH were shown in SI.

2.7 Electron transport chain (ETC) disruption upon CuO NPs exposure

The cells were treated with rotenone (Sigma, 10 μmol/L), anytimycin A (Sigma, 10 μmol/L), sodium cyanide (NaCN, Sigma, 1 mmol/L), and thenoyltrifluoroacetone (TTFA, Sigma, 10 μmol/L) for 0.5 h, respectively. After that, the plant cells (5×10^5 cells/mL) were added into CuO NPs suspension, with the final CuO NPs concentration at 12 mg/L. ROS contents were determined after 4 h exposure as mentioned in Section 2.5.

2.8 Gene analysis

BY-2 cells (5×10^5 cells/mL) were treated with CuO NPs (0 and 12 mg/L) for 4 h,

and then analysed by RNA-Seq. Briefly, total RNA of the cells was extracted using the mirVana miRNA Isolation Kit (Ambion-1561, Thermo Scientific) and then treated with DNase. The quality of extracted RNA was detected by Agilent 2100 Bioanalyzer (Agilent Technologies, Santa Clara, USA). The extracted RNA samples that located at the A_{260}/A_{280} range of 1.8-2.1 were identified as "purity", and "RNA Integrity Number (RIN) ≥7" was used for subsequent gene analysis. The results of above RNA quality assessment were listed in Table S2. A total of 4 μg RNA was used for library construction performed by Shanghai OE Biotech Company (Shanghai, China). The poly(A) mRNA was enriched by oligo (dT) magnetic beads. The mRNA was broken into short fragments to synthesize the first strand of cDNA by random hexamer-primer. DNA polymerase I was used to synthesize the second strand of cDNA, and then were connected using sequencing adapters. Then, the cDNA library was further sequenced on the illumina sequencing platform (Illumina HiSeq X10).

High-quality clean reads were acquired from raw reads by removing the reads containing adapter, or the reads containing ploy-N and low-quality reads by NGS QC Toolkit.[17] The obtained clean reads were mapped to reference *N. tabacum* genome by Bowtie 2 and Tophat (http://tophat.cbcb.umd.edu/).[18] The Cufflinks software was used to calculate the Fragments Per kb Per Million Reads (FPKM) values of the expression level of each gene,[19] and Htseq-count was used to count the read numbers that mapped to each gene.[20] Then, the differentially expressed genes were analysed using the DESeq functions estimateSizeFactors and nbinomTest to get the P-values and fold-change,[20] and "P-value < 0.05, fold-change > 2" were regarded as the threshold

for significant differentially expressed. Gene Ontology (GO) and Kyoto Encyclopedia of Gene and Genomes (KEGG) pathway analysis of differentially expressed genes were identified according to the hypergeometric test.[14] Because of little annotation information on *N. tabacum*, we analysed the orthologous genes of *N. tabacum* in *Arabidopsis* genome (http://www.arabidopsis.org) using BLAST approach.[21]

2.9 Quantitative real-time PCR Validation

To verify the accuracy of RNA-Seq, the expression of three genes (LOC107809014, LOC107826946, LOC107823778) which related to mitochondria were validated by quantitative real-time PCR (qRT-PCR). The same batch of the RNA samples for RNA-Seq analysis was employed as templates for reverse transcription using GeneAmp® PCR System 9700 (Applied Biosystems, USA). The obtained cDNAs were applied as qRT-PCR templates, and the reaction was performed using LightCycler® 480 II Real-time PCR Instrument (Roche, Swiss). At the end of the PCR cycles, melting curve analysis was used to validate the specific generation of the PCR product. The primer sequences were synthesized by Generay Biotech. Co. (Shanghai, China) (Table S3). The expression levels of mRNA were calculated by the $2^{-\Delta\Delta Ct}$ method.

2.10 Statistical analysis

All experiments were run at least in triplicate. The data were presented as mean ± standard deviation. One-way ANOVA with a LSD test using SPSS statistics was employed to analyze the data on growth inhibition, ROS and enzyme activity. Symbol "*" means statistical significance at "$p < 0.05$" level.

3. Results and Discussion

3.1 NPs characterization and cell viability

Both TEM (Figure S1A, S1B) and SEM (Figure S1C, S1D) images showed that CuO NPs and BPs were spherical, and the sizes of individual CuO NPs and BPs were 30-40 nm and 1500-2500 nm, respectively. The surface areas of CuO NPs and BPs were 12.01 and 0.51 m^2/g, respectively (Table S4). Zeta potentials of CuO NPs (–11.8 mV) and BPs (–14.5 mV) were both negatively charged in the 1/2 MS medium. Hydrodynamic diameters of CuO NPs and BPs in medium were 238.4 and 2403 nm, respectively, which were larger than those in ultrapure water. The released Cu^{2+} concentrations released from both CuO NPs and BPs at 12 mg/L increased with increasing incubation time (0-36 h). After incubation for 36 h, the released Cu^{2+} concentration from CuO NPs was 0.73 mg/L, which was much higher than that (0.11 mg/L) from CuO BPs (Figure S2). During 36-h dissolution, the concentration of the released Cu^{2+} ions was lower than 0.8 mg/L. Therefore, to investigate the contribution of the released Cu^{2+} on total CuO NPs toxicity, Cu^{2+} concentration at 0.80 mg/L was chosen as Cu^{2+} treatment in the following toxicity test.

Cell viability was investigated as a function of CuO NPs concentrations (0-50 mg/L). The viability inhibition was not observed after 24-h exposure to CuO NPs at 0-1 mg/L (Figure 1A). The minimum inhibitory concentration (MIC) of CuO NPs was 2 mg/L, and a dose-dependent cell viability inhibition was clearly observed when the CuO NPs was higher than 2 mg/L. The 24-h EC_{50} of CuO NPs to BY-2 cells in the present work was calculated as 12 mg/L. As for the plant *Elsholtzia splendens*, the

EC_{50} value of CuO NPs was as high as 480 mg/L.[22] For seed germination, EC_{50}s of CuO NPs to radish, and cucumber were 398, and 228 mg/L, respectively.[23] All these EC_{50} values were higher than that observed in the present work, indicating that the plant cells were much sensitive to CuO NPs than the whole plants or their seeds. In addition, CuO NPs at "12 mg/L" was selected in the following experiments on CuO NPs translocation and related mechanistic investigation. Cell viabilities in the presence of NPs, BPs and Cu^{2+} as a function of exposure times were also investigated. Both BPs (12 mg/L) and Cu^{2+} (0.8 mg/L) first promoted the growth of cells (0-4 h), and then decreased the cell viability (Figure 1B). For all the exposure times, CuO NPs (12 mg/L) had much stronger toxicity relative to CuO BPs (12 mg/L) and the dissolved Cu^{2+} ions (0.8 mg/L) ($p < 0.05$), clearly showing the "nano" effect of CuO on the toxicity to plant cells. Moreover, for Cu^{2+} at 9.6 mg/L (equal Cu content of CuO NPs at 12 mg/L), cell viability was sharply decreased to 2.9% after 2-h exposure and showed no recovery during 2-24 h exposure (Figure S3), suggesting that the toxicity of CuO NPs could be much stronger if the dissolution was enhanced in the medium or aquatic environments.

3.2 Translocation of CuO NPs in cells

Cellular uptake of CuO NPs was investigated using TEM (Figure 2). After exposure to CuO NPs for 12 h, the black dots extracellular and intracellular (vacuole) were observed (Figure 2A, marked with red square). EDS analysis showed that Cu contents (ranged from 1.41% to 12.79%, weight percentage) in these black dots were relatively higher, indicating the presence of CuO NPs (or their released Cu ions)

(Figure 2B). Further, it is confirmed that the black dots as marked with blue box in Figure 2B were indeed CuO NPs as detected with high resolution TEM (Figure S4). In addition, these Cu-containing dots were found on both mitochondria (Figure 2C, 2D) and cell wall after CuO NPs exposure (Figure 2E, 2F). The attachment and internalization of CuO NPs may result in further cytotoxicity.[24] For CuO BPs or Cu^{2+}-treated cells, the Cu-containing dots with the crystal plane of CuO were not found (Figure S5), indicating that CuO BPs could not be taken up by plant cells, and Cu^{2+} ions were unable to form CuO in the plant cells. Similarly, CuO NPs could be internalized into plant tissues such as roots[2], harvested seeds[1] after exposure of CuO NPs.

Subcellular changes of plant cells were further investigated (Figure 3). In comparison with the untreated cells (Figure 3A-3C), structural changes of cell wall, membrane and mitochondria (as indicated with red arrows) were found in the CuO NPs-treated cells (Figure 3D-3F). Cell wall became loose and the membrane became unclear and obscure after CuO NPs exposure. For mitochondria, the structure became swollen, and partial ridges of mitochondria disappeared. All these changes may be responsible for the observed growth inhibition of plant cells from CuO NPs (Figure 1). For CuO BPs or Cu^{2+} treatments, the damage on the structure of cell wall was not observed (Figure S5). For mitochondria, partial ridges after CuO BPs exposure were also unclear while they remained intact after Cu^{2+} exposure (Figure S5).

Endocytosis has been reported as a main pathway for the internalization of CuO NPs in mammalian cells.[25] Plant cells with a rigid cell wall received little attention on

the endocytosis. In this work, we used wortmannin as the endocytosis inhibitor, and found that intracellular Cu contents were significantly decreased after exposure to CuO NPs at 2 mg/L (45%) and 12 mg/L (32%) in comparison with the non-inhibitor treatment (Figure S6A). Wortmannin could suppress the activities of PI 3- and PI 4-kinases and the synthesis of phospholipids in plant cells,[26] and result in the decrease in internal vesicles. Our results clearly demonstrated that endocytosis was one of important pathways for CuO NPs internalization. Moreover, the vesicles at 300-500 nm were observed on the cell wall/membrane from TEM imaging (Figure S6B), and a high content of Cu (9.85%, weight percentage) was detected in the vesicle (Figure S6C). All these findings further confirmed endocytosis as an important pathway for CuO NPs internalization. Moreover, it is reported that vacuole with the functions of storage, waste disposal, maintenance of cell turgor and cell elongation,[27] is the destination of endocytosis, which was in good agreement with our findings that Cu-containing black dots located in vacuole (Figure 2B).

3.3 ROS, MDA, LDH generation and ETC

Total intracellular ROS upon exposure to CuO NPs (12 mg/L), CuO BPs (12 mg/L) and Cu^{2+} ions (0.8 mg/L) was shown in Figure 4A. For the CuO NPs treatment, ROS amount firstly increased to the maximum at 4 h, and then decreased, probably due to the self-repair of cells through anti-oxidative defense system. At 4-h exposure, total ROS in CuO NPs-treated plant cells was higher than that in CuO BPs and Cu^{2+} treatments ($p < 0.05$), indicating that the nanoparticulate CuO played a more important role in ROS generation than the released Cu^{2+} ions. It is known that

intracellular ROS mainly includes H_2O_2, $OH\cdot$ and $O_2\cdot^-$, which were further detected after 4-h exposure. For H_2O_2 and $OH\cdot$, the CuO NPs-treated cells had the highest contents, followed by Cu^{2+} and CuO BPs (Figure 4B, 4C), which was agreement with the order for total ROS (4-h exposure) as observed in Figure 4A. Excessive H_2O_2 in plant cells could result in oxidative stress and programmed cell death (PCD).[8] $OH\cdot$ could also play an important role in mediating intracellular oxidative stress.[28] As for $O_2\cdot^-$, no significant difference was observed among all the treatments (Figure 4D), indicating that H_2O_2 and $OH\cdot$ were the main species of oxygen radicals for the significant increase of oxidative stress. It should be noted that $O_2\cdot^-$ is very unstable, and mainly acts as one of the primary products of ROS. $O_2\cdot^-$ is easily to be transformed to H_2O_2 in mitochondria and cytoplasmic matrix[1], which may be an important source for H_2O_2 in plant cells after CuO NPs exposure.

The antioxidant defense system could be activated to protect against oxidative stress. After exposure to CuO NPs (12 mg/L) for 4 h, CAT activity was significantly triggered ($p < 0.05$) (Figure 5A), which can be explained by the excessive generation of intracellular H_2O_2 (Figure 4B). SOD activity after 4-h exposure followed the order: CuO NPs > Cu^{2+} $\approx$ CuO BPs > control. SODs are metal-containing enzymes that could eliminate $O_2\cdot^-$ radicals according to the following reaction: $2O_2\cdot^- + 2H^+ \rightarrow H_2O_2 + O_2$. The activation of SOD after CuO NPs exposure could explain the insignificant change in intracellular $O_2\cdot^-$ and significant increase in H_2O_2 as observed in Figure 4B.

Lipid peroxidation is an important indicator of membrane damage upon oxidative stress. As shown in Figure 5C, all the three treatments (CuO NPs, Cu^{2+},

CuO BPs) showed significantly higher MDA contents than that in the untreated cells, indicating the oxidative stress-induced membrane damage. We further investigated membrane leakage by detecting the extracellular LDH after 4-h exposure (Figure 5D). LDH in cytoplasm will be released outside the cells when membrane is incomplete or damaged. LDH level in cell medium is considered as the indicator of membrane integrity. Clearly, CuO NPs induced the highest extracellular content of LDH, suggesting the strongest membrane damage. Taken together, it can be concluded that CuO NPs induced the over-generation of intracellular ROS (H_2O_2 and OH·), and the oxidative stress led to the observed lipid peroxidation of membrane, thus causing membrane damage as indicated by significant LDH leakage.

ETC in the mitochondrial inner membrane contains complexes I (NADH dehydrogenase), II (Succinate dehydrogenase), III (Cytochrome *c* oxidoreductase), and IV (Cytochrome oxidase). Rotenone, TTFA, antimycin A and NaCN were the inhibitors of complexes I, II, III, and IV, respectively.[29] They can block the electron transfer at respective stages, and result in the leakage of electrons which could form ROS by combining with molecular oxygen. Figure 6 shows the ROS generation in the presence of NPs and different inhibitors. Each inhibitor alone caused the increase in ROS generation, confirming that these four inhibitors could effectively block ETC at respective stages by inhibiting complexes I-IV. For rotenone and antimycin A, ROS generation in plant cells after the co-incubation of inhibitors and CuO NPs was significantly higher than individual CuO NPs or inhibitor (Figure 6A, 6B). This indicated that CuO NPs could inhibit the activities of complexes I and III. Rotenone

could block the electrons from NADH to ubiquinone, and block electron transfer between iron-sulphur centre N-2 and ubiquinone.[30] Antimycin A inhibits the transfer of electron from ubisemiquinone to ubiquinol.[30] Overall, it can be concluded that CuO NPs blocked the transfers of electron from NADH to ubiquinone, from ubisemiquinone to ubiquinol in the present work. It is well known that complexes I and III of mitochondrial ETC are the main sites of $O_2^{\cdot -}$.[29] SOD dismutation can further reduce the moderately reactive $O_2^{\cdot -}$ to H_2O_2 in aqueous solution,[28] confirming the significant increase of intracellular H_2O_2 in CuO NPs-treated cells (Figure 4B). Moreover, H_2O_2 will react with Fe^{2+} and/or Cu^{+} in mitochondria to form OH·,[28] which is in good agreement with an increase in intracellular OH· after CuO NPs exposure. However, the co-incubation with both CuO NPs and the other two inhibitors (TTFA or NaCN) did not increase ROS generation in comparison with CuO NPs alone, suggesting that CuO NPs did not inhibit complex II and complex IV of mitochondrial ETC (Figure 6C, 6D). TTFA is the inhibitor of complex II by blocking the electron transfer from succinate to ubiquinone.[30] NaCN inhibits the oxidation of cyt a_3 by O_2, which could decrease oxygen production.[31] In conclusion, CuO NPs inhibited the activity of complex I and III, blocked the electron transfer from NADH to ubiquinone, and from ubisemiquinone to ubiquinol, inducing the generation of ROS and further leading to membrane damage (Figure S7).

3.4 GO enrichment analysis and KEGG annotation of transcripts

GO enrichment analysis

The differentially expressed genes in BY-2 cells upon CuO NPs exposure were

analysed using RNA-Seq. Information on the clean sequence data for both unexposed and CuO-treated cells were listed in Table S5. For each sample, the total mapped reads to *N. tabacum* genome were about 4.35 ~ 5.70 M, accounting for 87.9% ~ 89.0% of total reads by Tophat. The ratios of reads pair-mapped to total reads were 75.1% ~ 77.8% (Table S5). The hierarchy cluster analysis revealed that 2692 genes in BY-2 cells were differentially expressed after CuO NPs exposure (Figure S8A). Of these, 1132 genes were up-regulated, and 1560 genes were down-regulated, which were shown in the volcano plot (Figure S8B). To verify the accuracy of RNA-Seq, 3 differentially expressed genes (LOC107809014, LOC107826946, LOC107823778) were validated by qRT-PCR. The expression tendency of the tested genes by qRT-PCR was generally similar to that of the RNA-Seq (Figure S9 and Table S3), suggesting the reliable expression results generated by RNA-Seq.

GO enrichment analysis was used to better understand the functions of the differentially expressed genes after CuO NPs exposure. Figure 7 showed top 10 enriched GO terms of up-regulated and down-regulated genes in each GO category (biological process, cellular component, or molecular function). The enrichment scores (ESs) and P-values of the up-regulated and down-regulated GO terms were shown in Table S6 and S7, respectively. As for oxidative stress, among the top 10 GO terms of down-regulated genes in each GO category, “hydrogen peroxide catabolic process” (GO:0042744) and “response to oxidative stress” (GO:0006979) were involved in biological process (Figure 7A), and “peroxidase activity” (GO:0004601) was involved in the molecular function (Figure 7C), indicating that CuO NPs indeed

caused cellular oxidative stress. On the contrary, 2 terms including "response to hydrogen peroxide" (GO:0042542, Figure 7D) and "oxidoreductase activity" (GO:0016491, Figure 7F) were enriched in the top 10 up-regulated GO terms, which were involved in the categories of biological process and molecular function, respectively. The up-regulated expression of genes in these two terms suggested the antioxidative defense system was triggered during exposure.[32,33]

The GO terms related to mitochondria were analysed. In the cellular component category, "mitochondrial membrane" (GO:0031966), "mitochondrial inner membrane" (GO:0005743) and "mitochondrion" (GO:0005739) were involved in the top 10 enriched GO terms for the down-regulated genes (Figure 7B). Only 1 term related to "mitochondrion" (GO:0005739, Figure 7E) was identified in the top 10 enriched GO terms for the up-regulated genes. We did not find the GO terms that were related to mitochondria in the categories of biological process and molecular function. These results suggested that the structure of mitochondria was influenced after CuO NPs exposure, which is in good agreement with our TEM observations on the location of Cu-containing particles on cellular mitochondria (Figure 2D) and the changes of mitochondrial structure (Figure 3F). It should be noted that other GO terms of down-regulated genes involved in the mitochondrial ETC were also enriched although they were not included in the top 10 GO terms. These GO terms were "Respiratory chain" (GO:0070469, cellular component), "NAD binding" (GO:0051287, molecular function), "mitochondrial respiratory chain complex III assembly" (GO:0034551, biological process), "NAD(P)H dehydrogenase complex assembly" (GO:0010275,

biological process), "NADH dehydrogenase (ubiquinone) activity" (GO:0008137, molecular function), and "mitochondrial respiratory chain complex II", "succinate dehydrogenase complex (ubiquinone)" (GO:0005749, cellular component) were also enriched in GO terms of down-regulated genes. The down-regulation of genes in these GO terms indicated the dysfunction of mitochondria and possible disruption of mitochondrial ETC upon CuO NPs exposure.

The differentially expressed genes in mitochondrion-related GO terms were shown in Table S8. Thirty differentially expressed genes, including 19 down-regulated genes and 11 up-regulated genes were enriched in the mitochondrion-related GO terms. Among these genes, LOC107826946, LOC107819429, LOC107815753 and LOC107823778 (matched to S*DH2-1*, *COX11*, *PPOX2*, and *FTSH3* in *Arabidopsis*) that are closely related to mitochondrial ETC were further discussed. The down-regulation of *SDH2-1* gene suggested that the expression of the protein SDH2. SDH2, an iron-sulfur (Fe-S) protein containing three Fe-S clusters, is one subunits of succinate dehydrogenase (SDH, complex II),[34] and SDH could catalyze the oxidation of succinate to fumarate, and then reduce ubiquinone to ubiquinol without pumping protons across the mitochondrial inner membrane. Therefore, the down-regulation of *SDH2-1* gene may inhibit the reduction of ubiquinone to ubiquinol during mitochondrial electron transfer. The down-regulated of *COX11* gene suggested a decrease in biogenesis of cytochrome *c* oxidase.[35] The reduced cytochrome *c* could lead to the disruption of ubiquinol oxidation, and further block electron entry into complex III.[36] The down-regulation of *COX11* was also observed in *Saccharomyces*

cerevisiae when responding to abiotic stress (e.g., acetic acid).[37] *PPOX2*, an isoform of PPOX, was found in various plant species (e.g., *Arabidopsis*). PPOX is involved in the function of mitochondrial complex III.[38] The down-regulation of *PPOX2* indicated possible inhibition of complex III in mitochondria, which may be responsible for the generation of ROS as observed in the present work (Figure 4). *FTSH3* is localized on the inner membrane of plant mitochondria, and the catalytic site faces mitochondrial matrix. It is reported that the loss of *FTSH3* in *Arabidopsis* leads to a reduced activity of complex I.[39] In our work, the gene *FTSH3* was up-regulated upon CuO NPs exposure while complex I was inhibited from ETC inhibition data (Figure 6). It is speculated that the inhibition of complex I led to the over-expression of *FTSH3*, which has not been evidenced and needs further investigation.

KEGG analysis

The top 20 enriched KEGG pathways for the differentially expressed genes were shown in Figure S10. According to P-value, "glutathione metabolism" (ko00480) was the highest enriched KEGG pathways. Glutathione (GSH), an important antioxidant in plants, could eliminate intracellular H_2O_2 and defend oxidative stress in plant cells.[40,41] For the "glutathione metabolism" (ko00480) pathway, we identified 1 differentially expressed gene coded for glutathione transferase, 12 differentially expressed genes that coded for glutathione S-transferase, 1 for ascorbate peroxidases, 1 for glutathione synthase, and 1 for glutathione hydrolase (Table S9). The only differentially expressed gene (LOC107759987) for glutathione transferase was up-regulated after CuO NPs exposure. Glutathione transferase is known as a

detoxifying enzyme upon oxidative stress. There are 10 up-regulated genes (LOC107770509, LOC107779283, LOC107782951, LOC107782987, LOC107789895, LOC107795177, LOC107798067, LOC107800866, LOC107823949, LOC107831268) and 2 down-regulated genes (LOC107815009, LOC107779712) coded for glutathione S-transferase were identified, which catalysed glutathione to various electrophilic molecules. The differentially expressed gene that coded for ascorbate peroxidase was LOC107779974 (matched to *APX6* in *Arabidopsis*), which was up-regulated in BY-2 cells in the present work. *APX6* was reported to be up-regulated in *Arabidopsis* under oxidative stress induced by ionic Al,[14] which is in consistent with our finding. Also, the differentially expressed genes that coded for glutathione synthase (LOC107832748) and glutathione hydrolase (LOC107784134) were up- and down-regulated, respectively, implying an increase in glutathione level during 4-h CuO NPs exposure.

4. Conclusions

In this study, CuO NPs showed higher toxicity than CuO BPs and the dissolved Cu^{2+}. CuO NPs could be attached on the surface of plant cells, while some particles were transported into cytoplasm, mitochondria and vacuole via endocytosis. H_2O_2 and $OH^{\cdot}$ were the main ROS upon CuO NPs exposure, which caused lipid peroxidation, and finally led to membrane damage. It is explained that CuO NPs blocked the electron transport from NADH to ubiquinone to cytochrome *c* by inhibiting the activities of complexes I and III, resulting in the leakage of electrons and generation of ROS. Genomic study provided specific information on molecular mechanisms of

stress responded to CuO NPs. In this study, 2692 significantly differentially expressed genes were identified by RNA-Seq, including 1132 up-regulated and 1560 down-regulated genes (P-value < 0.05, fold-change > 2). These genes were further analysed with GO and KEGG. In the GO enrichment terms, the modulated terms related to oxidative stress, mitochondria and mitochondrial ETC played important roles in the toxicity of CuO NPs to plant cells. In addition, "GSH metabolism" was the most important enriched KEGG pathway. The information provided in this work shed light on the molecular mechanisms of nanotoxicity to plants.

Supplementary Information.

Ten figures and nine tables. This material is available free of charge via the Internet at http://pubs.rsc.org/.

Conflicts of interest

The authors report no conflict of interest.

Acknowledgements

This work was supported by NSFC (41530642, 41573092), NSF of Shandong Province (JQ201805), Aoshan Talents Program Supported by Qingdao National Laboratory for Marine Science and Technology (2015ASTP-0S04), Taishan Scholars Program of Shandong Province (tshw20130955), and USDA-NIFA Hatch program (MAS 00475).

References:

1 Z. Wang, L. Xu, J. Zhao, X. Wang, J. C. White and B. Xing, CuO Nanoparticle Interaction with *Arabidopsis thaliana*: Toxicity, Parent-Progeny Transfer, and Gene Expression, *Environ. Sci. Technol.*, 2016, 50, 6008-6016.

2 Z. Wang, X. Xie, J. Zhao, X. Liu, W. Feng, J. C. White and B. Xing, Xylem- and Phloem-Based Transport of CuO Nanoparticles in Maize (*Zea mays L.*), *Environ. Sci. Technol.*, 2012, 46, 4434-4441.

3 Y. Wang, R. Chen, Y. Hao, H. Liu, S. Song and G. Sun, Transcriptome analysis reveals differentially expressed genes (DEGs) related to lettuce (*Lactuca sativa*) treated by TiO_2/ZnO nanoparticles, *Plant Growth Regul.*, 2017, 83, 13-25.

4 J. Zhao, W. Ren, Y. Dai, L. Liu, Z. Wang, X. Yu, J. Zhang, X. Wang and B. Xing, Uptake, Distribution, and Transformation of CuO NPs in a Floating Plant *Eichhornia crassipes* and Related Stomatal Responses, *Environ. Sci. Technol.*, 2017, 51, 7686-7695.

5 L. Zhao, Q. Hu, Y. Huang, A. N. Fulton, C. Hannah-Bick, A. S. Adeleye and A. A. Keller, Activation of antioxidant and detoxification gene expression in cucumber plants exposed to a $Cu(OH)_2$ nanopesticide, *Environ. Sci.: Nano*, 2017, 4(8), 1750-1760.

6 M. L. López-Moreno, G. de la Rosa, J. Á Hernández-Viezcas, H. Castillo-Michel, C. E. Botez, J. R. Peralta-Videa and J. L. Gardea-Torresdey, Evidence of the differential biotransformation and genotoxicity of ZnO and CeO_2 nanoparticles on soybean (*Glycine max*) plants, *Environ. Sci. Technol.*, 2010, 44(19), 7315-7320.

7 L. Pagano, A. D. Servin, R. De La Torre-Roche, A. Mukherjee, S. Majumdar, J. Hawthorne, M. Marmiroli, E. Maestri, R. E. Marra, S. M. Isch, O. P. Dhankher, J. C. White and N. Marmiroli, Molecular response of crop plants to engineered nanomaterials, *Environ. Sci. Technol.*, 2016, 50(13), 7198-7207.

8 Z. Poborilova, R. Opatrilova and P. Babula, Toxicity of aluminium oxide nanoparticles demonstrated using a BY-2 plant cell suspension culture model, *Environ. Exp. Bot.*, 2013, 91, 1-11.

9 Y. Tang, R. He, J. Zhao, G. Nie, L. Xu and B. Xing, Oxidative stress-induced toxicity of CuO nanoparticles and related toxicogenomic responses in *Arabidopsis thaliana*, *Environ. Pollut.*, 2016, 212, 605-614.

10 P. M. Nair and I. M. Chung, Impact of copper oxide nanoparticles exposure on *Arabidopsis thaliana* growth, root system development, root lignificaion, and molecular level changes, *Environ. Sci. Pollut. R.*, 2014, 21, 12709-12722.

11 H. Yuan, S. Hu, P. Huang, H. Song, K. Wang, J. Ruan, R. He and D. Cui, Single walled carbon nanotubes exhibit dual-phase regulation to exposed Arabidopsis mesophyll cells, *Nanoscale Res. Lett.*, 2011, 6, 44.

12 S. Dang, Q. Liu, X. Zhang, K. He, C. Wang and X. Fang, Comparative cytotoxicity study of water-soluble carbon nanoparticles on plant cells, J. Nanosci. *Nanotechno.*, 2012, 12, 4478-4484.

13 D. M. Rhoads, A. L. Umbach, C. C. Subbaiah and J. N. Siedow, Mitochondrial reactive oxygen species. Contribution to oxidative stress and interorganellar signaling, *Plant Physiol.*, 2006, 141, 357-366.

14 Y. Jin, X. Fan, X. Li, Z. Zhang, L. Sun, Z. Fu, M. Lavoie, X. Pan and H. Qian, Distinct physiological and molecular responses in *Arabidopsis thaliana* exposed to aluminum oxide nanoparticles and ionic aluminum, *Environ. Pollut.*, 2017, 228, 517-527.

15 J. Hou, X. Liu, J. Wang, S. Zhao and B. Cui, Microarray-Based Analysis of Gene Expression in *Lycopersicon esculentum* Seedling Roots in Response to Cadmium, Chromium, Mercury, and Lead, *Environ. Sci. Technol.*, 2015, 49, 1834-1841.

16 H. Xun, X. Ma, J. Chen, Z. Yang, B. Liu, X. Gao, G. Li, J. Yu, L. Wang and J. Pang, Zinc oxide nanoparticle exposure triggers different gene expression patterns in maize shoots and roots, *Environ. Pollut.*, 2017, 229, 479-488.

17 R. K. Patel and M. Jain, NGS QC Toolkit: a toolkit for quality control of next generation sequencing data, *PLoS one*, 2012, 7, e30619.

18 D. Kim, G. Pertea, C. Trapnell, H. Pimentel, R. Kelley and S. L. Salzberg, TopHat2: accurate alignment of transcriptomes in the presence of insertions, deletions and gene fusions, *Genome Biol.*, 2013, 14, R36.

19 C. Trapnell, A. Roberts, L. Goff, G. Pertea, D. Kim, D. R. Kelley, H. Pimentel, S. L. Salzberg, J. L. Rinn and L. Pachter, Differential gene and transcript expression analysis of RNA-seq experiments with TopHat and Cufflinks, *Nat. Protoc.*, 2012, 7, 562-578.

20 S. Anders, P. T. Pyl and W. Huber, HTSeq - a Python framework to work with

high-throughput sequencing data, *Bioinformatics*, 2015, 31, 166-169.

21 C. Camacho, G. Coulouris, V. Avagyan, N. Ma, J. Papadopoulos, K. Bealer and T. L. Madden, BLAST+: architecture and applications, *BMC Bioinformatics*, 2009, 10, 421.

22 J. Shi, C. Peng, Y. Yang, J. Yang, H. Zhang, X. Yuan and T. Hu, Phytotoxicity and accumulation of copper oxide nanoparticles to the Cu-tolerant plant *Elsholtzia splendens*. *Nanotoxicology*, 2014, 8(2), 179-188.

23 S. G. Wu, L. Huang, J. Head, D. R. Chen, I. C. Kong and Y. J. Tang, Phytotoxicity of metal oxide nanoparticles is related to both dissolved metals ions and adsorption of particles on seed surfaces, *J. Pet. Environ. Biotechnol.*, 2012, 3(4), 126.

24 J. Zhao, X. Cao, X. Liu, Z. Wang, C. Zhang, J. C. White and B. Xing, Interactions of CuO nanoparticles with the algae *Chlorella pyrenoidosa*: adhesion, uptake, and toxicity, *Nanotoxicology*, 2016, 10, 1297-1305.

25 S. Behzadi, V. Serpooshan, W. Tao, M. A. Hamaly, M. Y. Alkawareek, E. C. Dreaden, D. Brown, A. M. Alkilany, O. C. Farokhzad and M. Mahmoudi, Cellular uptake of nanoparticles: journey inside the cell, *Chem. Soc. Rev.*, 2017, 46, 4218-4244.

26 K. Matsuoka, D. C. Bassham, N. V. Raikhel and K. Nakamura, Different sensitivity to wortmannin of two vacuolar sorting signals indicates the presence of distinct sorting machineries in tobacco cells, *J. Cell. Biol.*, 1995, 130, 1307-1318.

27 M. J. Marcote, F. Gu, J. Gruenberg and F. Aniento, Membrane transport in the endocytic pathway: animal versus plant cells, *Protoplasma*, 2000, 210, 123-132.

28 S. S. Gill and N. Tuteja, Reactive oxygen species and antioxidant machinery in abiotic stress tolerance in crop plants, *Plant Physiol. Bioch.*, 2010, 48, 909-930.

29 H. P. Indo, M. Davidson, H.-C. Yen, S. Suenaga, K. Tomita, T. Nishii, M. Higuchi, Y. Koga, T. Ozawa and H. J. Majima, Evidence of ROS generation by mitochondria in cells with impaired electron transport chain and mitochondrial DNA damage, *Mitochondrion*, 2007, 7, 106-118.

30 J. G. Zhang, F. A. Nicholls-Grzemski, M. A. Tirmenstein, and M. W. Fariss, Vitamin E succinate protects hepatocytes against the toxic effect of reactive oxygen species generated at mitochondrial complexes I and III by alkylating agents, *Chem-Biol. Interact.*, 2001, 138, 267-284.

31 M. Ghyczy, C. Torday, J. Kaszaki, A. Szabó, M. Czóbel and M. Boros, Hypoxia-Induced Generation of Methane in Mitochondria and Eukaryotic Cells - An Alternative Approach to Methanogenesis, *Cell. Physiol. Biochem.*, 2008, 21, 251-258.

32 J. T. Van Dongen and F. Licausi, Low-oxygen stress in plants. *Springer Verlag Gmbh*, 2016, pp 25.

33 Y. Shu, J. Zhang, Y. Ao, L. Song and C. Guo, Analysis of the Thinopyrum elongatum transcriptome under water deficit stress, *Int. J. Genomics*, 2015.

34 S. Huang and A. H. Millar, Succinate dehydrogenase: the complex roles of a simple enzyme, Curr. Opin. *Plant Biol.*, 2013, 16, 344-349.

35 M. Bode, M. W. Woellhaf, M. Bohnert, M. v. d. Laan, F. Sommer, M. Jung, R. Zimmermann, M. Schroda and J. M. Herrmann, Redox-regulated dynamic interplay between Cox19 and the copper-binding protein Cox11 in the intermembrane space of mitochondria facilitates biogenesis of cytochrome *c* oxidase, *Mol. Biol. Cell.*, 2015, 26, 2385-2401.

36 Q. Chen, E. J. Vazquez, S. Moghaddas, C. L. Hoppel and E. J. Lesnefsky, Production of Reactive Oxygen Species by Mitochondria CENTRAL ROLE OF COMPLEX III, *J. Biol. Chem.*, 2003, 278, 36027-36031.

37 B. Li and Y. Yuan, Transcriptome shifts in response to furfural and acetic acid in *Saccharomyces cerevisiae*, *Appl. Microbiol. Biot.*, 2010, 86, 1915-1924.

38 M. D. Ferrer, A. Sureda, P. Tauler, C. Palacin, J. A. Tur and A. Pons, Impaired lymphocyte mitochondrial antioxidant defences in variegate porphyria are accompanied by more inducible reactive oxygen species production and DNA damage, *Brit. J. Haematol.*, 2010, 149, 759-767.

39 K. Marta, G. Marta, U. Adam and J. Hanna, The significance of *Arabidopsis* AAA proteases for activity and assembly/stability of mitochondrial OXPHOS complexes, *Physiol. Plantarum*, 2007, 129, 135-142.

40 L. Wang, H. Yang, R. Liu and G. Fan, Detoxification strategies and regulation of oxygen production and flowering of *Platanus acerifolia* under lead (Pb) stress by transcriptome analysis, *Environ. Sci. Pollut. R.*, 2015, 22, 12747-12758.

41 S. K. Yadav, Heavy metals toxicity in plants: an overview on the role of glutathione and phytochelatins in heavy metal stress tolerance of plants, *S. Afr. J. Bot.*, 2010, 76, 167-179.

Figures:

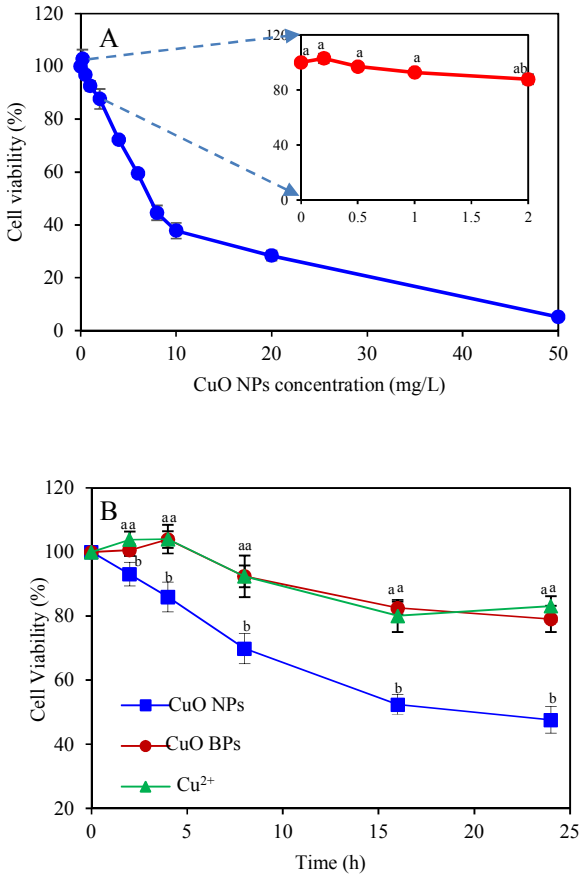

Figure 1. The viability of BY-2 cells after exposure to CuO NPs, BPs, and Cu^{2+}. (A) Cell viability after treated with CuO NPs at different concentrations (0, 0.2, 0.5, 1, 2, 4, 6, 8, 10, 20, 50 mg/L) for 24 h. The inserted figure in panel (A) showed the decrease of cell viability as a function of CuO NPs concentrations (0.2-2 mg/L). (B) BY-2 cells exposed to CuO NPs, BPs, Cu^{2+} with different times. In panel B, the concentrations of CuO NPs, BPs and Cu^{2+} were 12, 12 and 0.8 mg/L, respectively (n=3). Different letters (a-b) indicate significant difference among different treatment at a given concentration ($p < 0.05$, LSD, n=3).

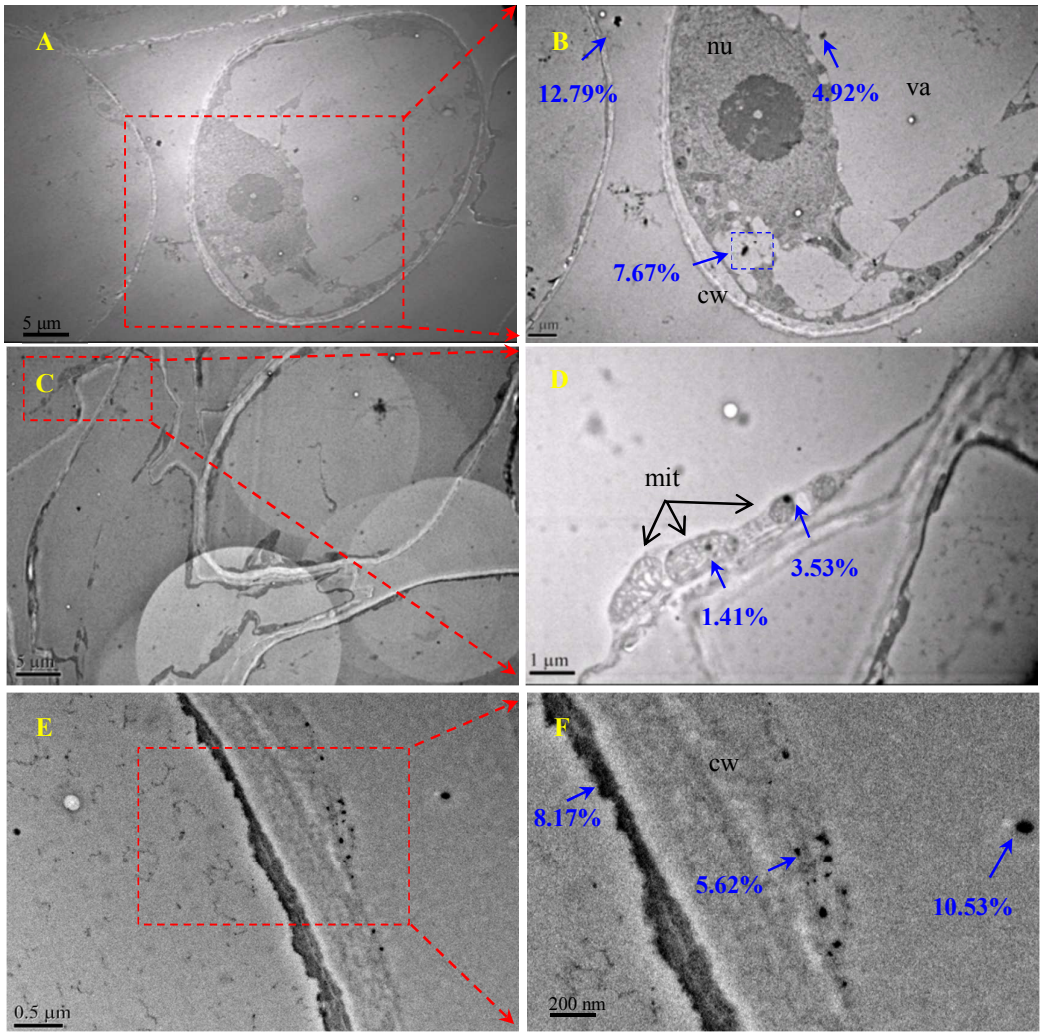

Figure 2. Distribution of CuO NPs in BY-2 cells after exposure to CuO NPs (12 mg/L) for 12 h. Panels B, D, and F are enlarged from panels A, C, and E, respectively. Blue arrow: Cu components; blue digital mark: the content of Cu atoms confirmed by EDS; cw: cell wall; nu: nuclear; va: vacuole; mit: mitochondria.

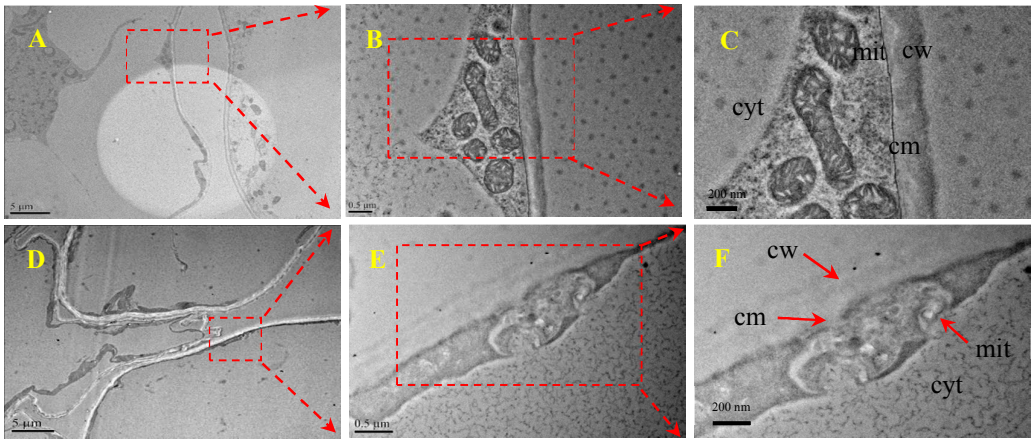

Figure 3. TEM observations of the subcellular changes of BY-2 cells. (A) untreated cells, (D) cells treated with 12 mg/L CuO NPs for 12 h. (B), (C) and (E), (F) were enlarged views of (A) and (D), respectively. Red arrow: the subcellular changes of the CuO NPs-treated cells; cw: cell wall; cm: cell membrane; cyt: cytoplasm; mit: mitochondria.

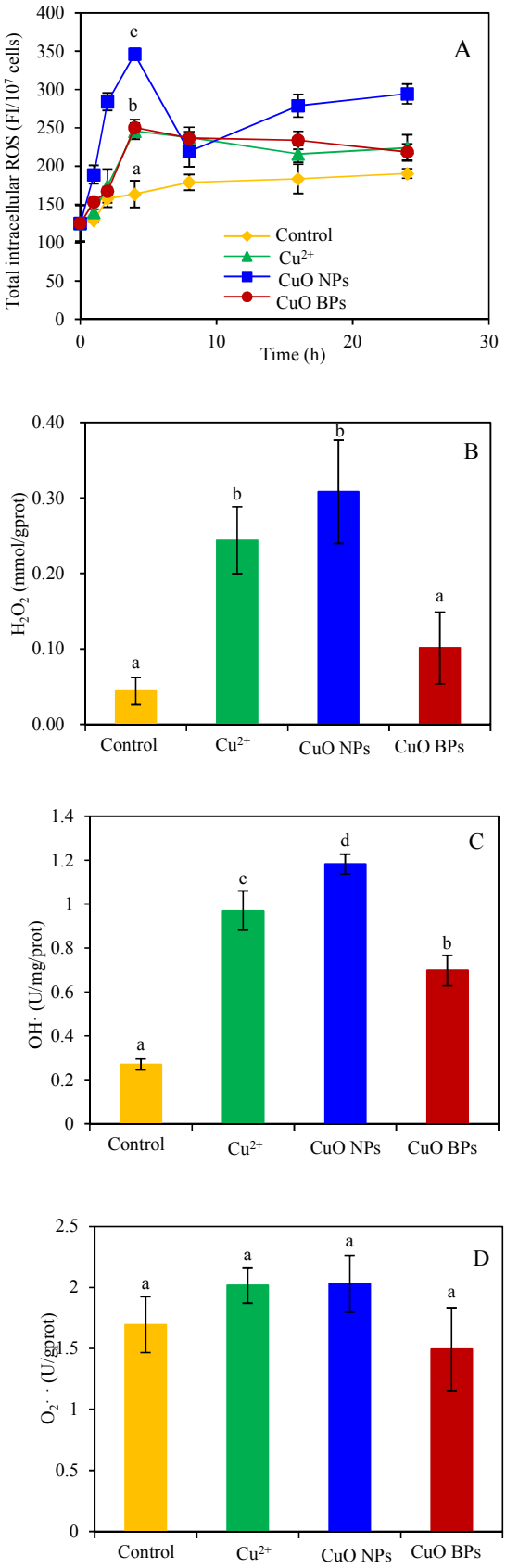
A
Total intracellular ROS (FI/10^7 cells)
Time (h)
Control
Cu2+
CuO NPs
CuO BPs
B
H2O2 (mmol/gprot)
C
OH· (U/mg/prot)
D
O2·- (U/gprot)

Figure 4. Generation of ROS in BY-2 cells after CuO NPs (12 mg/L), BPs (12 mg/L) and Cu^{2+} (0.8 mg/L) exposure. (A) Generation of total intracellular ROS as a function of exposure time (0-24 h). (B), (C), (D): Generation of H_2O_2, OH· and O_2^{-}· after 4-h exposure. Different letters (a–d) indicate significant difference among different treatments ($p < 0.05$, LSD, n=3).

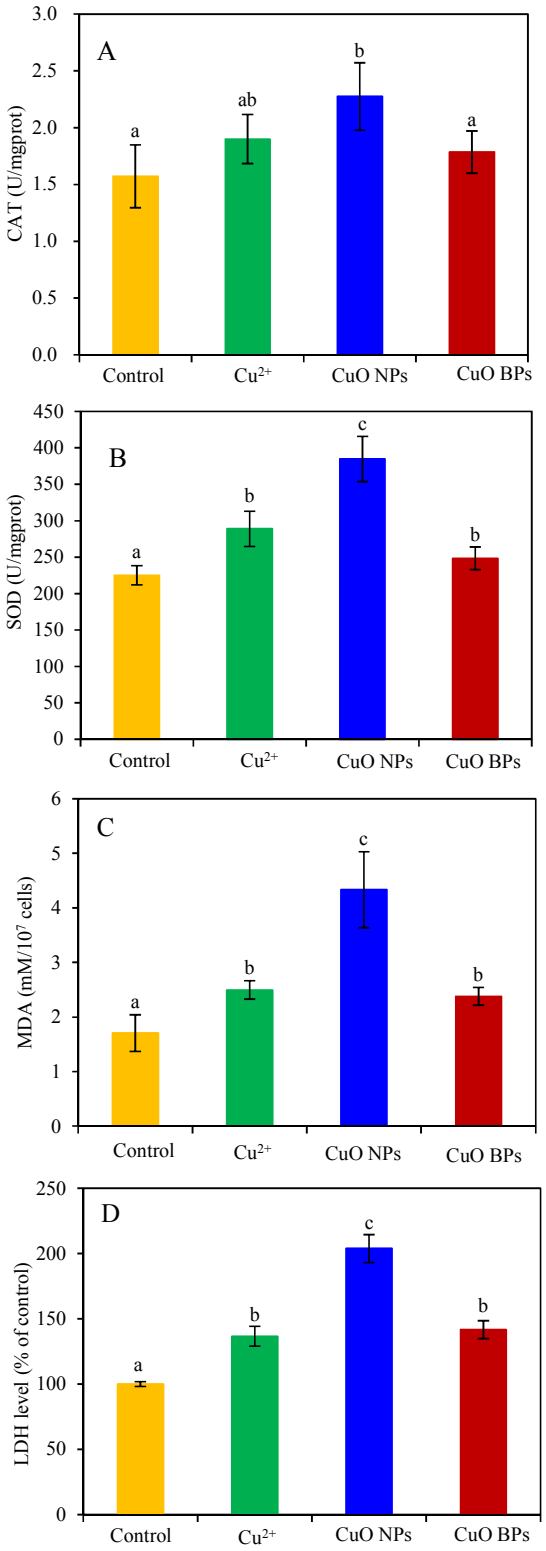

Figure 5. Activity changes of key antioxidant enzyme and membrane damage of BY-2 cells after exposure to CuO NPs (12 mg/L), CuO BPs (12 mg/L) or Cu^{2+} (0.8 mg/L) for 4 h. (A): CAT

(catalase); (B): SOD (superoxide dismutase). (C) MDA contents of BY-2 cells after CuO NPs exposure; (D) LDH leakage of BY-2 cells. In each panel, the letters (a–c) indicate significant difference among different treatments ($p < 0.05$, LSD, n=3).

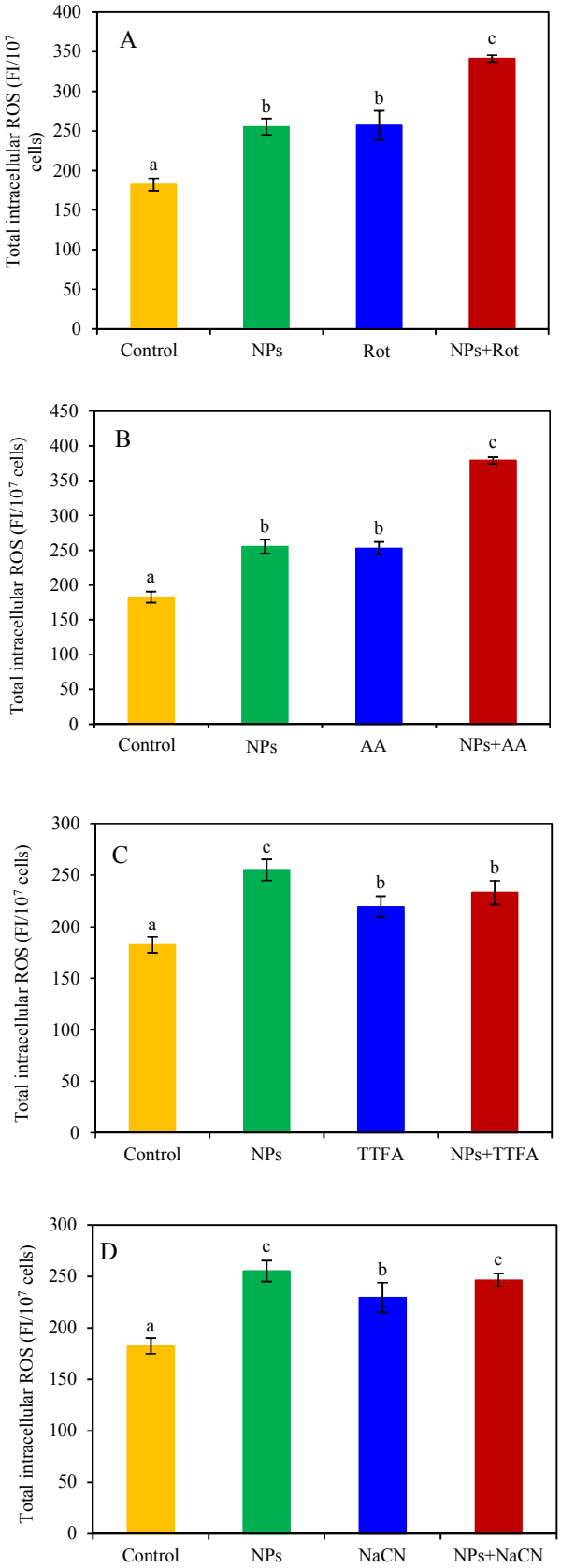
A
Total intracellular ROS (FI/10^7 cells)
400
350
300
250
200
150
100
50
0
a
b
b
c
Control
NPs
Rot
NPs+Rot
B
Total intracellular ROS (FI/10^7 cells)
450
400
350
300
250
200
150
100
50
0
a
b
b
c
Control
NPs
AA
NPs+AA
C
Total intracellular ROS (FI/10^7 cells)
300
250
200
150
100
50
0
a
c
b
b
Control
NPs
TTFA
NPs+TTFA
D
Total intracellular ROS (FI/10^7 cells)
300
250
200
150
100
50
0
a
c
b
c
Control
NPs
NaCN
NPs+NaCN

Figure 6. Effects of rotenone (A), antimycin A (B), TTFA (C) and NaCN (D) on ROS generation of plant cells induced by CuO NPs (12 mg/L). Data followed by different letters (a–c) indicate significant difference among different treatments ($p < 0.05$, n=3). In each panel, Rot and AA are the abbreviations of rotenone and antimycin, respectively.

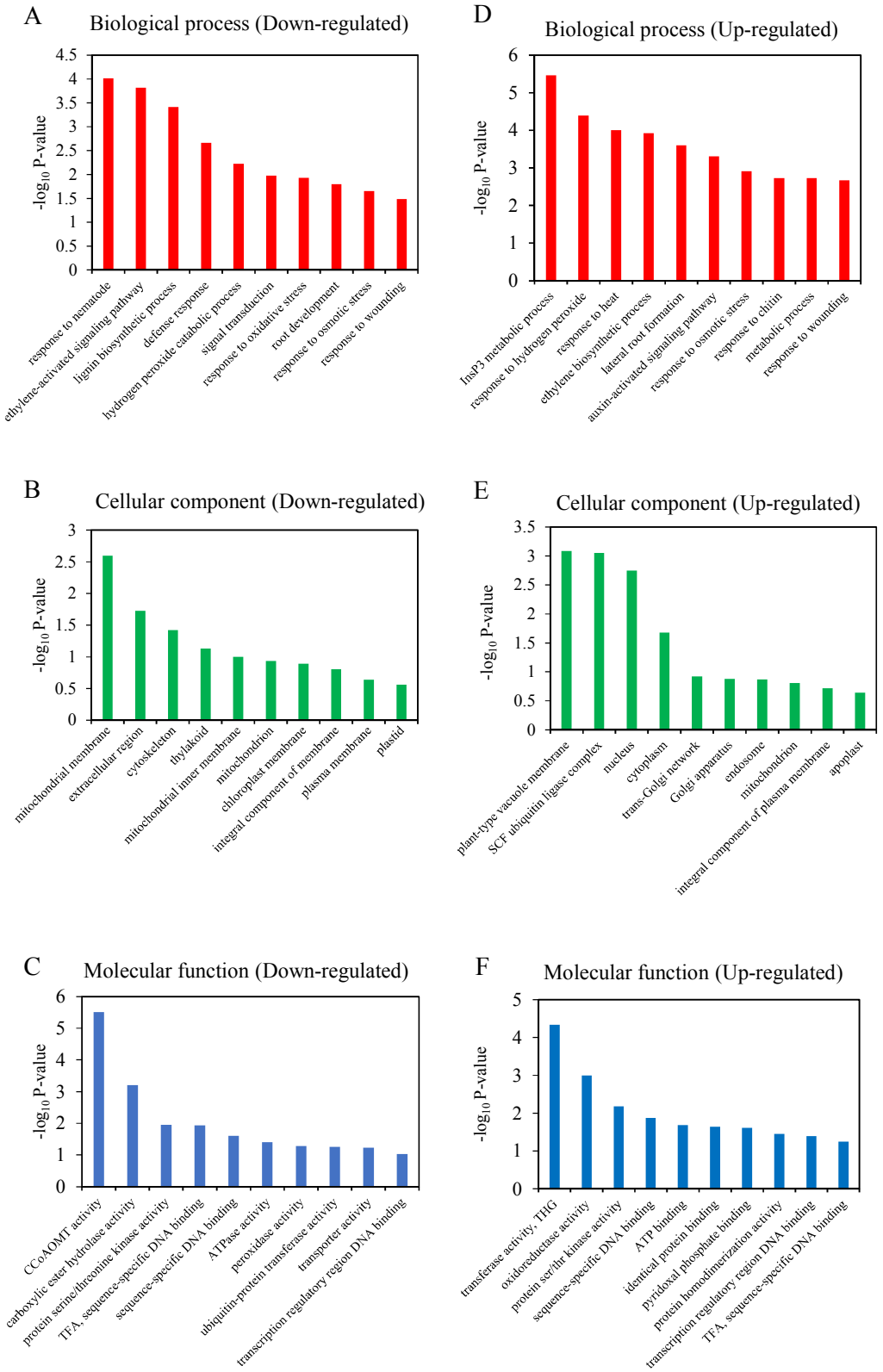

Figure 7. GO functional categories for the differentially expressed genes of BY-2 cells after CuO NPs exposure. The top 10 enriched GO terms of down-regulated (A, B, C) and up-regulated (D, E,

F) genes were categorized to biological process, cellular component and molecular function, respectively. In the figure, CCoAOMT, TFA, InsP3, Thr, and Ser stand for caffeoyl-CoA O-methyltransferase, transcription factor activity, inositol trisphosphate, Threonine, and Serine, respectively.

Graphic Abstract